Complex model for fatigue damage development

Cite as: AIP Conference Proceedings **2312**, 050015 (2020); https://doi.org/10.1063/5.0035517
Published Online: 19 November 2020

I. S. Nikitin, N. G. Burago, A. D. Nikitin, and B. A. Stratula

Complex Model for Fatigue Damage Development

I S Nikitin, N G Burago, A D Nikitin and B A Stratula

Institute for computer aided design of RAS, 2-ya Brestskaya st., 123056, Moscow, Russia

Corresponding author: i_nikitin@list.ru

Abstract. A complex kinetic model of damage development under cyclic loading is proposed to describe the process of fatigue failure. Two criteria that imply different micro-crack development types are used in the model. A numerical method for calculating crack-like zones up to macro fracture is proposed. The results of numerical fatigue experiments are presented; the operability of the model and calculation algorithm is shown. It was shown that the presence of two criteria that use different types of crack nucleation may result in cases when one of the criteria leads to crack growth while the other one does not and vice versa. Under a complex stress state in the proposed complex model the natural implementation of any of the considered crack development mechanisms is possible. Cracks of different types may develop simultaneously in various parts of a specimen.

INTRODUCTION

In recent decades, entire classes of criteria have been constructed that relate the number of cycles before the initiation of fatigue damage (micro-cracks) with the amplitudes and maximum values in the cycle (or average) that characterize the uniform stress-strain state of the working part of the specimen in a fatigue test. A large number of stress criteria are based on a direct generalization of the S-N Wöhler-type curves described by Basquin-type relations [1] for fatigue tests. Reviews on this topic are given in [2–4].

In this paper we study the processes of fatigue damage zones development using the damage theory approach dating back to [5,6]. In the application to the cyclic loading and fatigue failure problems this approach was implemented in [7,8]. A complex model for the development of fatigue failure with use of the evolutionary equation for the damage function is proposed. It is associated with two different fatigue criteria. These criteria describe different crack development types. The model parameters are determined for various fatigue failure modes – low-cycle and high-cycle fatigue (LCF, HCF).

The following scheme of the amplitude fatigue curve is used. Up to value $N \sim 10^3$ the regime of repeated-static loading with amplitude slightly differing from the static tensile strength σ_B is realized. Further the fatigue curve (Wöhler curve) describes the modes of the LCF-HCF up to $N \sim 10^7$ with an asymptotic approach to the fatigue limit σ_u.

It should be noted that at present there is an idea of an explicit division of the classic Wöhler branch into two parts – in fact, the LCF and the HCF. The boundary of this transition region is determined not by the value of *N*, but by the loading amplitude that is equal to the yield strength of the material σ_T [9], since this means a change of the physical mechanism of fatigue failure. In addition, the boundary of the repeated-static range $N \sim 10^3$ is rather arbitrary. It is also specified in [9] depending on the strength and plastic characteristics of the material. However, in this paper we will keep the suggestion of the proposed model of damage development based on the scheme described above.

Proceedings of the X All-Russian Conference
AIP Conf. Proc. 2312, 050015-1–050015-8; https://doi.org/10.1063/5.0035517
Published by AIP Publishing. 978-0-7354-4052-4/$30.00

The model associated with the two well-known criteria for multiaxial fatigue failure is proposed. These criteria imply different micro-crack development types. The first one describes the fatigue failure associated with the tensile micro-cracks development. It is the stress-based Smith–Watson–Topper criterion [10] described in [11], in which the amplitudes of maximum tensile stress play a decisive role in the development of fatigue damage. The second one describes the fatigue failure associated with the shear micro-cracks development. It is the stress-based Carpinteri–Spagnoli–Vantadori criterion [12]. Under a complex stress state in the proposed complex model the natural implementation of any of the considered crack development mechanisms is possible. Cracks of different types may develop simultaneously in various parts of a specimen.

For numerical simulation a simple holed specimen is used. Different loading regimes are applied to study the simultaneous impact of the multiple criteria.

KINETIC EQUATION FOR DAMAGE IN LCF-HCF MODE

Various criteria use different stress combinations to calculate an equivalent stress value. Some of them are based on normal stress components of a stress state while other are based on shear components. In this paper we are going to implement two criteria simultaneously: one is based on a tensile micro-cracks which is the stress-based Smith–Watson–Topper [11], the other one is based on a shear micro-cracks and implements the notion of a critical plane which is the stress-based Carpinteri–Spagnoli–Vantadori [12].The considered model develops the damage model in case of cyclic loads, presented in [13] for the description of damages during dynamic loading.

Generic equations

At first, let us introduce some variables that are used later.

We can write a generic fatigue fraction criterion corresponding to the left branch of the bimodal fatigue curve in the following form:

$$\sigma_{eq} = \sigma_u + \sigma_L N^{-\beta} \tag{1}$$

From the condition of repeated-static fracture up to values of $N \sim 10^3$ by the method [4] it is possible to obtain the value $\sigma_L = 10^{3\beta}(\sigma_B - \sigma_u)$. In these formulas σ_B is the static tensile strength of the material, σ_u is the classic fatigue limit of the material during a reverse cycle (asymmetry coefficient of the cycle R = -1), β is power index of the left branch of the bimodal fatigue curve.

From the fatigue fracture criterion we obtain the number of cycles before fracture at uniform stressed state:

$$N = 10^3 \left[(\sigma_B - \sigma_u) / (\sigma_{eq} - \sigma_u) \right]^{1/\beta} \tag{2}$$

In order to describe the process of fatigue damage development in the LCF-HCF mode, a damage function $0 \le \psi(N) \le 1$ is introduced, which describes the process of gradual cyclic material failure. When $\psi = 1$ a material particle is considered completely destroyed. Its Lame modules become equal to zero. The damage function ψ as a function on the number of loading cycles for the LCF-HCF mode is described by the kinetic equation:

$$\mathrm{d}\psi / \mathrm{d}N = B\psi^{\gamma} / (1 - \psi^{\alpha}) \tag{3}$$

where α and $0 < \gamma < 1$ are the model parameters that determine the rate of fatigue damage development. The choice of the denominator in this two-parameter equation, which sets the infinitely large growth rate of the zone of complete failure at $\psi \to 1$, is determined by the known experimental data on the kinetic growth curves of fatigue cracks, which have a vertical asymptote and reflects the fact of their explosive, uncontrolled growth at the last stage of macro fracturing.

An equation for damage of a similar type was previously considered in [8], its numerous parameters and coefficients were determined indirectly from the results of uniaxial fatigue tests. In our case, the coefficient B is determined by the procedure that is clearly associated with the selected criterion for multiaxial fatigue failure of one type or another. It has the following form.

The number of cycles to complete failure N at $\psi = 1$ is found from the equation for damage for a uniform stress state:

$$\left[\psi^{1-\gamma}/(1-\gamma)-\psi^{(1+\alpha-\gamma)}/(1+\alpha-\gamma)\right]\Big|_0^1 = B\,N\Big|_0^N, \qquad (4)$$
$$N=\alpha/(1+\alpha-\gamma)/(1-\gamma)/B$$

By calculating the value N from the fracture criterion (2) and from the solution of the equation for damage (4), we obtain the expression for the coefficient B :

$$B=10^{-3}\left[(\sigma_{eq}-\sigma_u)/(\sigma_B-\sigma_u)\right]^{1/\beta}\alpha/(1+\alpha-\gamma)/(1-\gamma) \qquad (5)$$

where the value σ_{eq} is determined by the selected mechanism of fatigue failure and the corresponding multiaxial criterion (1).

When $\sigma_{eq}\le\sigma_u$ fatigue failure does not occur, when $\sigma^{eq}\ge\sigma_B$ it occurs instantly.

Smith–Watson–Topper criterion

The criterion of multiaxial fatigue failure in the LCF-HCF mode with the development of normal-stress micro-cracks (stress-based SWT) corresponding to the left branch of the bimodal fatigue curve has the form:

$$\sqrt{\langle\sigma_{1_{\max}}\rangle\Delta\sigma_1/2}=\sigma_u+\sigma_L N^{-\beta} \qquad (6)$$

where σ_1 is the largest principal stress, $\Delta\sigma_1$ is the spread of the largest principal stress per cycle, $\Delta\sigma_1/2$ is its amplitude. According to the chosen criterion only tensile stresses lead to failure, so it has the value $\langle\sigma_{1_{\max}}\rangle=\sigma_{1_{\max}}H(\sigma_{1_{\max}})$. Here $H(x)$ stands for the Heaviside step function.

Let us put down the following notation:

$$\sigma^n=\sqrt{\langle\sigma_{1_{\max}}\rangle\Delta\sigma_1/2} \qquad (7)$$

Here the upper index n stands for denotation and should not be considered as a power.

Carpinteri–Spagnoli–Vantadori criterion

The criterion of multiaxial fatigue failure in the LCF-HCF mode, including the concept of a critical plane (stress-based CSV), corresponding to the left branch of the bimodal fatigue curve has the form:

$$\sqrt{(\langle\Delta\sigma_n\rangle/2)^2+k_c^2(\Delta\tau_n/2)^2}=\sigma_u+\sigma_L N^{-\beta} \qquad (8)$$

where $\Delta\tau_n/2$ is the amplitude of the tangential stress on the plane (critical), where it reaches its maximum value, $\Delta\sigma_n/2$ is the amplitude of the normal (tensile) stress on the critical plane, $\langle\Delta\sigma_n\rangle=\Delta\sigma_n H(\sigma_{n_{\max}})$. Here, the shear fatigue limit τ_u for a pulsating cycle is additionally introduced at a cycle asymmetry coefficient of $R=-1$. In a simplified formulation, we can approximately accept $k_c\approx\sigma_u/\tau_u$ and $k_c\approx\sqrt{3}$. This criterion includes the mechanism of fatigue fracture with the formation of shear micro-cracks.

Let us put down the following notation:

$$\sigma^\tau=\sqrt{(\langle\Delta\sigma_n\rangle/2)^2+3(\Delta\tau_n/2)^2} \qquad (9)$$

Here the upper index τ stands for denotation and should not be considered as a power.

ALGORITHM FOR FATIGUE DAMAGE DEVELOPMENT CALCULATION

The Ansys software was used to calculate the loading cycle of a deformable specimen, supplemented by a code to calculate the damage equation and changes of elasticity modulus.

General Approach to Damage Function

To integrate the equation $d\psi/dN = B\psi^{\gamma}/(1-\psi^{\alpha})$, the damage function approximation was applied at the k-node of the computational grid for given discrete values ψ_k^t at moments N^t and sought ψ_k^{t+1} at moments N^{t+1}.

To calculate the damage equation, the value $\alpha = 1-\gamma$ was chosen for which by analytic integration an explicit expression for $\psi_k^{t+1}(\psi_k^t, \Delta N^t)$ can be obtained:

$$\left[\psi^{1-\gamma}/(1-\gamma) - \psi^{2(1-\gamma)}/2/(1-\gamma)\right]\Big|_{\psi_k^t}^{\psi_k^{t+1}} = B_k\, N\Big|_{N^t}^{N^{t+1}} \tag{10}$$

With the denotations $(\psi_k^{t+1})^{1-\gamma} = x$, $q = 2(1-\gamma)B_k\Delta N^t + (\psi_k^t)^{1-\gamma} - 2(\psi_k^t)^{2(1-\gamma)}$ and $\Delta N^t = N^{t+1} - N^t$ the equation transforms to $x^2 - 2x + q = 0$ and its valid root $x = 1 - \sqrt{1-q} < 1$.The damage parameter depends on the increment of the number of cycles ΔN^t as:

$$\psi_k^{t+1} = \left(1 - \sqrt{1 - \left[2(1-\gamma)B_k\Delta N^t + (\psi_k^t)^{1-\gamma} - 2(\psi_k^t)^{2(1-\gamma)}\right]}\right)^{1/(1-\gamma)} \tag{11}$$

Here increment value ΔN^t defined as follows. Based on the stress state calculation data, the coefficient B_k is calculated for each node. After that, for each node, the following values are calculated

$$\Delta\tilde{N}_k^t = \left[\psi^{1-\gamma}/(1-\gamma) - \psi^{2(1-\gamma)}/2/(1-\gamma)\right]\Big|_{\psi_k^t}^{1} / B_k \tag{12}$$

corresponding to the number of cycles at which in the node k from its current level of damage and equivalent stress complete destruction will be achieved (damage is equal to 1). If the damage level in the considered node is less than the threshold ψ_0 (threshold $\psi_0 = 0.95$ is selected), then the value for this node $\Delta\tilde{N}_k^t$ is multiplied by a factor of 0.5. Otherwise, it is multiplied by a factor of 1. Thus, the step of incrementing the number of cycles for a given node is $\Delta N_k^t = 0.5(1 + H(\psi_k^t - 0.95))\Delta\tilde{N}_k^t$. Of all the ΔN_k^t values the smallest one is selected. The increment of the number of loading cycles for the calculation of the entire specimen is $\Delta N^t = \min\limits_k \Delta N_k^t$. For each node, based on its current level of damage and equivalent stress, a new level of damage is estimated taking into account the calculated increment ΔN^t.

Criterion Selection

At each node there are not one but two B values, namely B^n and B^τ. From (5) they have the forms:

$$\begin{aligned} B^n &= 10^{-3}\left[\langle\sigma^n - \sigma_u\rangle/(\sigma_B - \sigma_u)\right]^{1/\beta}\alpha/(1+\alpha-\gamma)/(1-\gamma), \\ B^\tau &= 10^{-3}\left[\langle\sigma^\tau - \sigma_u\rangle/(\sigma_B - \sigma_u)\right]^{1/\beta}\alpha/(1+\alpha-\gamma)/(1-\gamma) \end{aligned} \tag{13}$$

It means there are 2 damage values $\psi^n = f(B^n)$ and $\psi^\tau = f(B^\tau)$. At every step both ψ^n and ψ^τ are calculated for every node, then they are compared with each other at every node. When and where one of them becomes greater than 0 the other value is fixed to 0. It means that at every node the process that started first (via either SWT or SCV) prevails over the other one until the end of calculation process. Before the decisive moment both processes have equal rights to be the first one.

Material Properties Change

All elements are sorted out, for each of them the most damaged node is searched and according to its damage the mechanical properties of the element are adjusted:

$$\lambda(\psi_k^t) = \lambda_0(1 - \kappa\psi_k^t), \quad \mu(\psi_k^t) = \mu_0(1 - \kappa\psi_k^t) \tag{14}$$

Those elements that belong to nodes with damage $\psi = 1$ are removed from the calculation area and form a localized zone (crack-like) of completely destroyed material. The calculation ends when the boundaries of a completely damaged region exit to the specimen surface (macro destruction) or the evolution of this region stops.

CALCULATION RESULTS

A series of numerical experiments were conducted to determine the impact of the proposed scheme on fatigue behavior of a specimen. Our goal was to study a multi-axial case namely a torsion-compression stress-state.

Initial Conditions

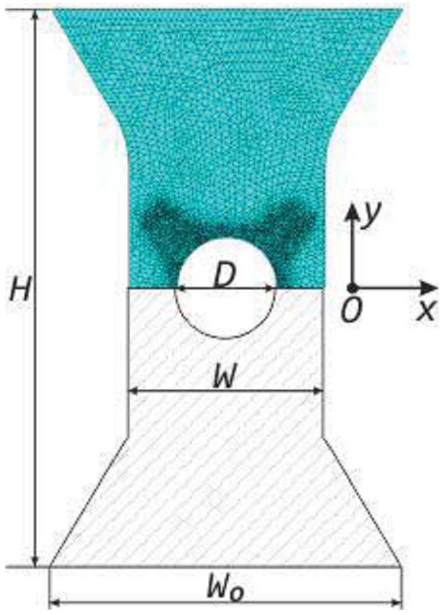

FIGURE 1. Specimen geometry

All tests were conducted on a holed specimen, Fig. 1. Width at boundaries W_0 = 107 mm, main width W = 60 mm, height H = 170 mm, hole diameter D = 30 mm, thickness T = 1.75 mm. It should be noted that the numerical experiments were performed in three-dimensional space.

Due to symmetry of the specimen over Ox axis we decided to perform calculations only on the top half of the specimen. At that part the finite element grid is shown. We applied deformations at the top boundary of the specimen; due to its symmetry quasi-same deformations but in the opposite direction were applied at the bottom boundary, so at the cross-section along Oxz there were no transverse (along Oy axis) deformations. In all numerical experiments all loads are in the same phase and their asymmetry ratios R = 0.5.

Plate material – titanium alloy with strength and fatigue parameters σ_B = 1135 MPa, σ_u = 330 MPa, β = 0.31. Elasticity modulus of intact alloy are λ_0 = 77 GPa, μ_0 = 44 GPa.

Shear is applied along Ox axis which means that a positive shear deformation value corresponds to shift in the right-hand side direction. Tension and compression are applied along Oy axis. It means that a positive tension deformation corresponds to shift in the up direction and a positive compression deformation corresponds to shift in the down direction.

Numerical Experiments

The first numerical experiment was on pure tension. The tension amplitude was 0.2 mm. The stress distribution before the crack initiation is presented at Fig. 2-a; the corresponding amount of cycles $N = 1.1 \cdot 10^5$. The stress distribution and the crack are presented at Fig. 2-b. The crack is marked with arrows, their direction show the type of the crack development process. Here it was grown via the development of normal-stress micro-cracks; the corresponding amount of cycles $N = 1.5 \cdot 10^5$.

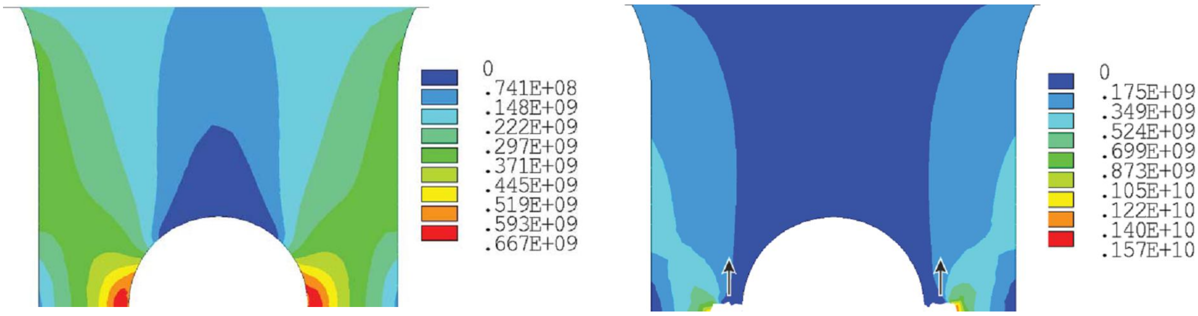

a) Before the crack initiation b) Crack growth process

FIGURE 2. The numerical experiment on pure tension

The second numerical experiment was on pure shear. The shear amplitude was 0.5 mm. The stress distribution before the crack initiation is presented at Fig. 3-a; the corresponding amount of cycles $N = 6.2 \cdot 10^5$. The stress distribution and the crack are presented at Fig. 3-b. Again the crack was grown via the development of normal-stress micro-cracks; the corresponding amount of cycles $N = 7.2 \cdot 10^5$.

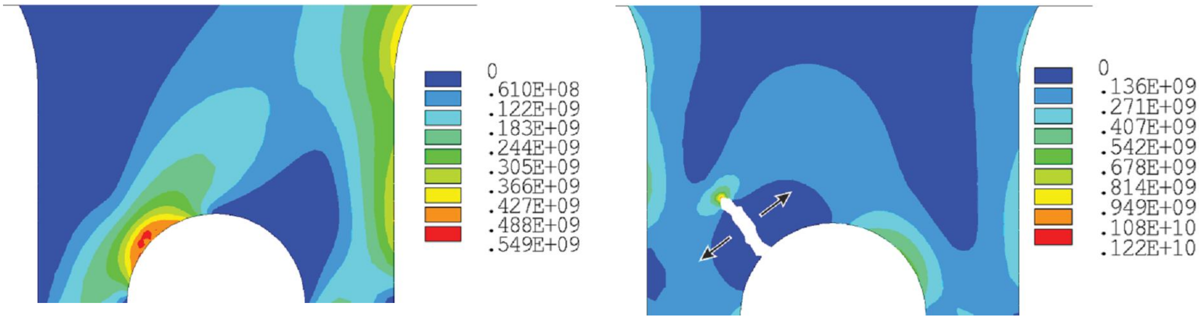

a) Before the crack initiation b) Crack growth process

FIGURE 3. The numerical experiment on pure shear

The third numerical experiment comprises compression and shear. The compression amplitude was 0.06 mm and the shear amplitude was 0.5 mm. The stress distribution before the crack initiation is presented at Fig. 4-a; the corresponding amount of cycles $N = 9.0 \cdot 10^5$. The stress distribution and the crack are presented at Fig. 4-b. Here are two crack, the left one was grown via the development of normal-stress micro-cracks while the right was grown via the shear-stress micro-cracks; the corresponding amount of cycles $N = 9.8 \cdot 10^5$.

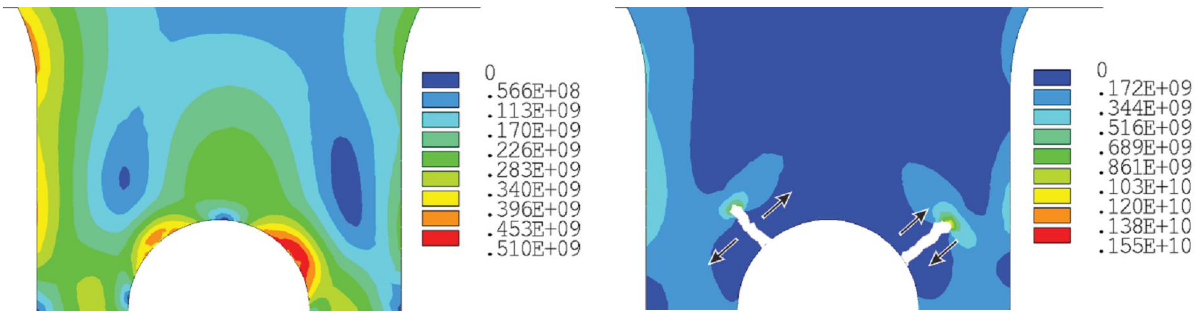

a) Before the crack initiation b) Crack growth process

FIGURE 4. The numerical experiment on compression and shear

The fourth and the last numerical experiment again comprises compression and shear, but with different amplitudes. The compression amplitude was 0.1 mm and the shear amplitude was 0.5 mm. The stress distribution before the crack initiation is presented at Fig. 5-a; the corresponding amount of cycles $N = 3.2 \cdot 10^5$. The stress distribution and the crack are presented at Fig. 5-b. There is only one crack and it was grown via the shear-stress micro-cracks; the corresponding amount of cycles $N = 4.3 \cdot 10^5$.

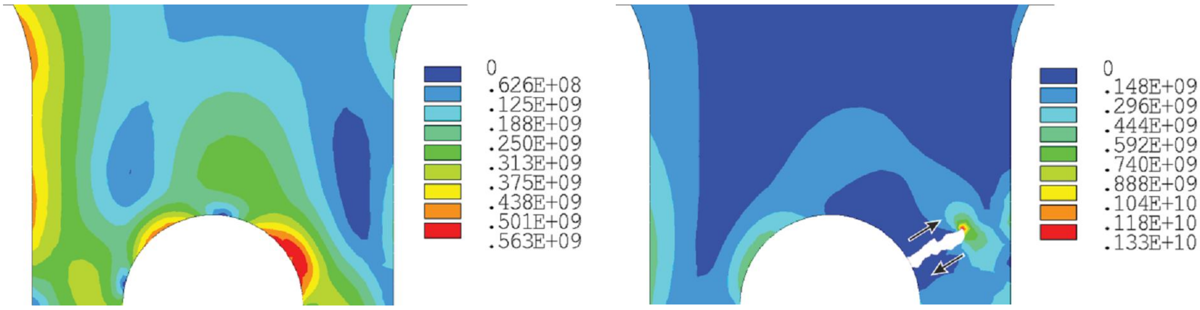

a) Before the crack initiation b) Crack growth process

FIGURE 5. The numerical experiment on compression and shear

CONCLUSIONS

A kinetic model of cyclic loading damage development is proposed to describe the fatigue fracture process development. To determine the coefficients of the kinetic equation of damage, the combination of the two known criteria of multiaxial fatigue fracture were used namely the SWT criterion and the CSV criterion. It was shown that the presence of two criteria that use different regimes of crack nucleation may result in cases when one of the criteria leads to crack growth while the other one does not and vice versa. Under a complex stress state in the proposed complex model the natural implementation of any of the considered crack development mechanisms is possible. Cracks of different types may develop simultaneously in various parts of a specimen.

ACKNOWLEDGMENTS

The study was carried out with a grant from the Russian Science Foundation (project No. 19-19-00705).

REFERENCES

1. Basquin, O.H., “The exponential law of endurance tests”, Proc of the American society for testing and material **10**, 625–630 (1910).
2. Meggiolaro, M.A., Miranda, A.C., de Castro, J., “Comparison among fatigue life prediction methods and stress-strain models under multiaxial loading”, Proceedings of 19th Int. Congress of Mech. Eng.
3. Karolczuk, A., Papuga, J., Palin-Luc, T., “Progress in fatigue life calculation by implementing life-dependent material parameters in multiaxial fatigue criteria”, Int. J. of fatigue **134**, 1–13 (2020).
4. Bourago, N.G., Zhuravlev, A.B., Nikitin, I.S., “Models of multiaxial fatigue fracture and service life estimation of structural elements”, Mechanics of Solids **46**, 828–838 (2011).
5. Kachanov, L.M., “O vremeni razrushenija v usloviyah polzuchestyIzv”, AN SSSR OTN **8**, 26–31 (1958).
6. Rabotnov, J.N., “O mechanizme dlitel’nogo razrushenia. Voprosi prochnosti materialov i konstrukcij”, AN SSSR OTN, 5–7 (1959).
7. J. Lemaitre and J.L. Chaboche, *Mechanics of solid materials* (Cambridge: Cambridge University Press, 1994), p. 582.
8. Marmi, A.K., Habraken, A.M., Duchene, L., “Multiaxial fatigue damage modeling at macro scale of Ti6Al4V alloy”, Int. J. of fatigue **31**, 2031–2040 (2009).

9. Shanyavskiy, A.A., Soldatenkov, A.P., "The fatigue limit of metals as a characteristic of the multimodal fatigue life distribution for structural materials", Procedia Structural Integrity **23**, 63–68 (2019).
10. Smith, R.N., Watson, P., Topper, T.H., "A stress-strain parameter for the fatigue of metals", J. of Materials **5**, 767–778 (1970).
11. Gates, N., Fatemi, A., "Multiaxial variable amplitude fatigue life analysis including notch effects", Int. J. of fatigue **91**, 337–351 (2016).
12. Carpinteri, A., Spagnoli, A., Vantadori, S., "Multiaxial assessment using a simplified critical plane based criterion", Int. J. of Fatigue **33**, 969–976 (2011).
13. Burago, N.G., Nikitin, I.S., Nikitin, A.D., Stratula, B.A., "Algorithms for calculation damage processes", Frattura ed Integrità Strutturale **49**, 212–224 (2019).